



RESEARCH ARTICLE

10.1002/2014WR015597

Key Points:

- Bankfull shear stress varies continuously with grain size across transport mode
- An empirical relation for depth, slope, and grain size is used as closure
- This framework applies to modern and ancient alluvial rivers on Earth

Supporting Information:

- Newly compiled data set for modern alluvial channels
- Description of data set and sources

Correspondence to:

B. McElroy,
bmcelroy@uwyo.edu

Citation:

Trampush, S. M., S. Huzurbazar, and B. McElroy (2014), Empirical assessment of theory for bankfull characteristics of alluvial channels, *Water Resour. Res.*, 50, 9211–9220, doi:10.1002/2014WR015597.

Received 17 MAR 2014

Accepted 20 OCT 2014

Accepted article online 27 OCT 2014

Published online 5 DEC 2014

Empirical assessment of theory for bankfull characteristics of alluvial channels

S. M. Trampush¹, S. Huzurbazar², and B. McElroy¹

¹Department of Geology and Geophysics, University of Wyoming, Laramie, Wyoming, USA, ²Department of Statistics, University of Wyoming, Laramie, Wyoming, USA

Abstract We compiled a data set of 541 bankfull measurements of alluvial rivers (see supporting information) and used Bayesian linear regression to examine empirical and theoretical support for the hypothesis that alluvial channels adjust to a predictable condition of basal shear stress as a function of sediment transport mode. An empirical closure based on channel slope, bankfull channel depth, and median grain size is proposed and results in the scaling of bankfull Shields stress with the inverse square root of particle Reynolds number. The empirical relationship is sufficient for purposes of quantifying paleohydraulic conditions in ancient alluvial channels. However, it is not currently appropriate for application to alluvial channels on extraterrestrial bodies because it depends on constant-valued, Earth-based coefficients.

1. Introduction

Configurations of alluvial channels on Earth appear to be driven by the complementary tasks of transporting fluids and solids [Leopold and Maddock, 1953; Langbein and Leopold, 1964; Parker, 1978a, 1978b]. Resistance to flow of water offered by granular materials, channel boundaries, and other obstacles results in transfer of momentum to sediments as well as momentum losses through dynamic pressure gradients [Einstein, 1950]. This ultimately leads to an interplay between discharge of water, movement of sediment, and ultimately the forms of channels. It has been argued that noncohesive sand and gravel systems are organized such that their bankfull geometries are related to the hydrodynamic properties of a representative portion of their sediment loads [García *et al.*, 2000; Parker *et al.*, 2007; Wilkerson and Parker, 2011]. It has been further argued that shear stresses experienced by sediments at bankfull discharge are roughly balanced by the load to be carried such that channels with different modal grainsizes have distinct boundary stresses. In this scenario, sand is just barely suspended at bankfull while gravel, experiencing a distinct shear stress at bankfull, is transported very near the threshold of motion [Parker, 1978a, 1978b; Dade and Friend, 1998]. These arguments support the notion that rivers organize bankfull shear stress around a geomorphic threshold driven by the dominant transport mode of bed sediment [Talling, 2000; Church, 2002; Jerolmack and Brzinski, 2010]. More recent additions of data from rivers with intermediate grain sizes [Wilkerson and Parker, 2011; Hajek and Wolinsky, 2012] suggest that the relationship between particle Reynolds number and Shields stress is not well explained by two stable bankfull Shields stresses based on grain category (i.e., sand or gravel) and is more appropriately conceptualized as a continuously varying function across grain sizes.

With a database of 225 independent data points in sandy channels, Wilkerson and Parker [2011] (Figure 1, after their Figure 2) found empirically that bankfull Shields stress scales linearly with the inverse square root of particle Reynolds number. To further elucidate this empirical relationship, we have accumulated another 316 data points from literature reporting hydraulic geometry and grain size surveys collocated with river gauging stations. The data are presented as supporting information. From analysis of the new data set, we highlight (1) that the empirical relationship for bed slope, median grain size, and bankfull channel depth appropriately explains the variance of bankfull Shields stress with particle Reynolds number, (2) that there is no indication that the relationship between bankfull shear stress and median grain size of the bed is discontinuous at the sand/gravel transition (i.e., there is no apparent sand/gravel threshold in stress states), (3) that this relationship is appropriate for estimating slopes of ancient alluvial channels from their preserved deposits, and (4) that this relationship is restricted in its current form to applications for alluvial river channels on Earth.

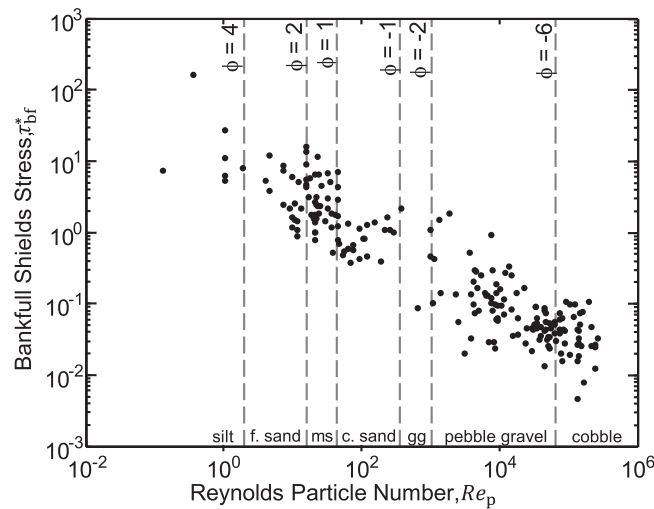


Figure 1. Relationship between bankfull Shields stress and particle Reynolds number containing 225 data points (black points) as presented by Wilkerson and Parker [2011] (after their Figure 2). Gray lines are divisions between major grain size categories. Note the scarcity of data in the very coarse sand to granule gravel size range.

2. Theory

In order to investigate potential universality of the organization of alluvial channels (or quasi-universality *sensu* [Wilkerson and Parker, 2011]), their physical systems must be appropriately nondimensionalized [Parker *et al.*, 2007]. Water flowing in alluvial channels applies stresses to granular materials, and the ability of flowing fluids to move particles is appropriately captured by Shields stress [e.g., Julien, 1998; García, 2007]. Specifically, Shields stress is the magnitude of basal shear stress applied by flow normalized to the submerged weight of median sized grains, and it is denoted by τ_* :

$$\tau_* = \frac{\tau_b}{\rho R g D_{50}}, \quad (1)$$

where τ_b (kg/ms^2) is the basal shear stress, ρ (kg/m^3) is the density of water, R (unitless) is the submerged specific gravity of sediment, g (m/s^2) is gravitational acceleration, and D_{50} (m) is the median size of bed material. In the numerator, the basal shear stress is defined under conditions of steady, uniform flow as $\tau_b = \rho g R S$, where R (m) is a channel's hydraulic radius (area of channel cross section divided by the wetted perimeter) and S (unitless) is the slope of the water surface. Because alluvial channels generally have width

to depth ratios much larger than unity, R can be approximated by average flow depth, H (m), without loss of fidelity in the relationship (1) [Parker, 1978b]. Total basal shear stresses are therefore regularly approximated by the depth-slope product scaled by density and gravity, usually written as $\tau_b = \rho g H S$.

The approach outlined above does not separate form drag from skin friction in hydraulic resistance. Form drag is defined as the resistance to flow attributed to normal forces and their derived pressure gradients caused by obstacles to flow [Einstein, 1950]. In order to remove this component from total boundary shear stress, it would be necessary to quantify flow resistance due to bed forms, bars, channel curvature, and objects such as large woody debris. Furthermore, it would be necessary to tie this quantification directly to local conditions including bankfull depth, channel slope, and median grain size of bed sediment. While

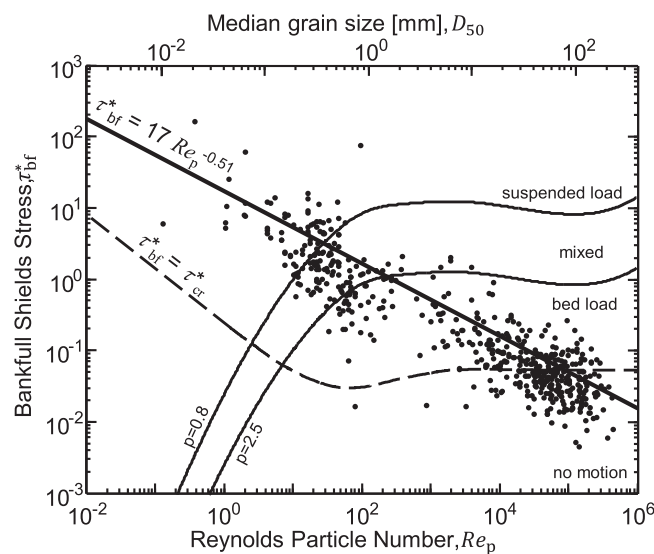


Figure 2. Bankfull Shields stress plotted against particle Reynolds number calculated from record in our reported data set (black points) with thick solid line showing semiempirical relationship for τ_{*bf}^* and Re_p . Thick line and equation derived from a Bayesian regression using equation (5). Thin, solid black curves are lines of constant Rouse number, p , giving approximate boundaries between modes of sediment transport [Bagnold, 1973; van Rijn, 1984; Julien, 1998]. Specifically, Rouse curves are determined by relating shear velocity at bankfull to bankfull Shields stress and fall velocity to particle Reynolds number. Thin, dashed black curve is Shields curve defining the threshold of particle motion estimated by methods described in García [2007] and references therein. Note that although gravel is largely transported as bed load during bankfull conditions, sand is transported nearly equally as bed load and in suspension.

substantial progress has been made to understand the component of resistance from sandy bed forms [Engelund and Fredsoe, 1982], there is no general theory to predict skin friction as a function of these other physical parameters. As a consequence, it is likely that there is systematic variability of form drag longitudinally down channels and across all channels as a function of channel slope or bankfull depth. Although an attempt to account for this is made by Wilkerson and Parker [2011], they appropriately note that theirs is a broad brush characterization of nongrain-scale resistance. We have omitted this complication largely because no formulation exists that would reduce uncertainty in our estimates of the stresses experienced by bed sediments at bankfull across the range of alluvial channels. However, it will be important to consider this simplification when interpreting our analysis and the relationship between bankfull Shields stress and particle Reynolds number.

Wolman and Miller [1960] argue based on total geomorphic work that a dominant water discharge can be determined by the product of its work magnitude and its frequency of occurrence relative to all other discharges. In alluvial channels, this is generally termed the effective discharge. Empirically, this discharge approximately fills the channel that it constructs [Dunne and Leopold, 1978], and its level is termed bankfull depth, H_{bf} . Alternatives to effective discharge have been proposed to quantify morphologic relationships to sediment transport and water discharge. Vogel et al. [2003] provided the basis for fractional load discharges, and Doyle et al. [2007] argued for the concept of functionally equivalent discharge. Doyle et al. [2007] also demonstrate a close correspondence between effective discharge and bankfull discharge in a range of settings except flashy and ephemeral streams. The analysis presented here is limited to the extent that effective discharge and bankfull discharge are equivalent or nearly so. If channel geometries are generated by flows at bankfull conditions, then the relevant stress for moving sediments to form a channel must be the boundary shear stress at bankfull, $\tau_{bf} = \rho g H_{bf} S$. Substituting this expression into equation (1) gives definition for bankfull Shields stress, τ_{bf}^* ,

$$\tau_{bf}^* = \frac{H_{bf} S}{RD_{50}} \tag{2}$$

In addition to characterizing hydraulics of alluvial systems to investigate their unifying organization, sediment properties and loads must also be appropriately summarized. This is paramount to understanding connections between driving stresses and sediment behavior. Following Yalin [1972], Ackers and White [1973], and more recently Wilkerson and Parker [2011], we define a particle Reynolds number, Re_p , such that particle size is nondimensionalized through the submerged specific gravity of the granular material, gravitational acceleration, and viscosity of the fluid,

$$Re_p = \frac{\sqrt{Rg}}{\nu} D_{50}^{3/2} \tag{3}$$

where ν (m^2/s) is kinematic viscosity.

Bankfull Shields stress, τ_{bf}^* , and particle Reynolds number, Re_p , can be related analytically through median grain size, D_{50} , using equations (2) and (3),

$$\tau_{bf}^* = \left(\frac{\sqrt{g}}{R\nu} \right)^{2/3} H_{bf} S Re_p^{-2/3} \tag{4}$$

Wilkerson and Parker [2011] report an empirical scaling of $\tau_{bf}^* \sim Re_p^{-1/2}$. In contrast, in this theoretical relationship, it appears that $\tau_{bf}^* \sim Re_p^{-2/3}$. However, the relationship (4) was derived by relating the definitions of bankfull Shields stress, τ_{bf}^* , and particle Reynolds number, Re_p , through median grain size, D_{50} . If channel slope, S , or bankfull depth, H_{bf} , depend on median grain size, then the exponent on particle Reynolds number does not accurately reflect its scaling with bankfull Shields stress. In order to resolve this issue and close a theoretical relationship between τ_{bf}^* and Re_p , we must determine the relationship between H_{bf} , S , and D_{50} .

Based on the results of Mueller et al. [2005], Parker et al. [2007] speculate on a relationship between S and H_{bf}/D_{50} , and they use it to account for form drag in gravel bedded rivers. Paola and Mohrig [1996] also propose a relationship between channel slope, bankfull depth, and median grain size for gravel bed rivers that takes the form $S \sim D_{50}/H_{bf}$. Rather than prescribe the scaling between S , H_{bf} , and D_{50} , we start with an unconstrained, purely empirical relationship such that

Table 1. Summary of Posterior Distributions of Coefficients^a

Parameter	Mean	Standard Deviation	2.5%	25%	50%	75%	97.5%
<i>Equation (5)</i>							
Intercept (α_0)	-2.08	0.036	-2.14	-2.10	-2.08	-2.05	-2.01
$\log D_{50}$ effect (α_1)	0.254	0.016	0.222	0.244	0.254	0.266	0.287
$\log H_{bf}$ effect (α_2)	-1.09	0.044	-1.18	-1.12	-1.09	-1.06	-1.00
<i>Equation (8)</i>							
Intercept (γ_0)	1.24	0.14	0.95	1.15	1.24	1.34	1.50
$\log S$ effect (γ_1)	0.078	0.038	0.00	0.054	0.079	0.10	0.15
$\log Re$ effect (γ_2)	-0.51	0.014	-0.48	-0.50	-0.51	-0.52	-0.54

^aDistributions presented as percentiles, e.g., 2.5% of the estimated coefficients for α_0 were less than -2.14.

$$\log S = \alpha_0 + \alpha_1 \log D_{50} + \alpha_2 \log H_{bf}. \tag{5}$$

This closes the theoretical relationship empirically, and it results in a surface in \mathbb{R}^3 that fully describes the interrelation of these three physical parameters of alluvial systems.

To accomplish this empirical closure, equation (5) is rearranged to be an expression for bankfull flow depth

$$\log H_{bf} = -\frac{\alpha_0}{\alpha_2} - \frac{\alpha_1}{\alpha_2} \log D_{50} + \frac{1}{\alpha_2} \log S, \tag{6}$$

and substituting it into the definition for bankfull Shields stress results in

$$\log \tau_{bf}^* = -\frac{\alpha_0}{\alpha_2} - \log R - \left(\frac{\alpha_1}{\alpha_2} + 1\right) \log D_{50} + \left(\frac{1}{\alpha_2} + 1\right) \log S. \tag{7}$$

We then relate bankfull Shields stress to particle Reynolds number (equations (3) and (7)) through median grain size to obtain

$$\log \tau_{bf}^* = \gamma_0 + \gamma_1 \log S + \gamma_2 \log Re_p, \tag{8}$$

where $\gamma_0 = \frac{\alpha_0}{\alpha_2} - \log R + \frac{2}{3} \left(\frac{\alpha_1}{\alpha_2} + 1\right) \log \left(\frac{\sqrt{Rg}}{v}\right)$, $\gamma_1 = \left(\frac{1}{\alpha_2} + 1\right)$, and $\gamma_2 = -\frac{2}{3} \left(\frac{\alpha_1}{\alpha_2} + 1\right)$. This equation represents a semiempirical solution to the relationship of bankfull Shields stress and particle Reynolds number using their definitions and an empirical relationship for the scaling of the physical variables, channel slope, bankfull depth, and median grain size. We investigate the relationship in equation (5) using a new compilation of alluvial channel data including 225 previously compiled data points and 316 newly compiled data points. We then substantiate the semiempirical relationship of bankfull Shields stress and particle Reynolds number equation (8) by applying the results of a linear regression for equation (5) within a Bayesian framework using the combined data set of 541 measurements.

3. Methods

3.1. Data Compilation

Many U.S. government agencies have released reports in the last 10 years on bankfull geometry of rivers from across North America. For this work, data compiled from these reports were used to augment the *Wilkinson and Parker* [2011] data set from U.S. and global sources. To be included, individual locations must have the following information available: mean bed or water surface slope, bankfull water depth, and median grain size. Most of the compiled reports exist in digital formats, allowing easy data import with the aid of a text editor. For a few reports, data were entered into the data set by hand with subsequent quality checks for transcription errors. Locations excluded from the database have incomplete measurements or had data values visually estimated rather than directly measured.

The individual components of the data set have been collected with a variety of methods that have broad similarities; methodologies are generally based on those outlined by *Harrelson et al.* [1994], *Leopold* [1994], and *Rosgen* [1996] (supporting information, Table 1). Most of the surveys represent measurements on riffles in basins where less than 20% of the drainage area is classified as urban. No streams were included if they were known or reported to be ephemeral. Bankfull depth in most instances was measured from bankfull

indicators (e.g., topographic breaks in slope from the top of the bar to the flood plane, change in grain characteristics, or vegetation). Slope was generally measured from longitudinal surveys of the water surface or channel bed. Median grain sizes were mostly obtained in the field with a Wolman pebble count method for gravel bed rivers [Wolman, 1954] or by sampling and sieving for sand-bed rivers. Most median grain size values represent an average of multiple measurements. The included sites have more than 10 years of record for their associated stream gages. The minimum period of record was chosen to be 10 years to assure that the hydrographic record is substantially longer than the bankfull return period. This roughly assures that it would be possible to independently identify a bankfull discharge from a rating curve at the gage if necessary. Further information on the methods and criteria are included with the data set in the supporting information. Overall, these methods represent appropriate data collection techniques to estimate the parameters relevant to our objective, elucidating the universality of the relationship between bankfull Shields stress and particle Reynolds number.

3.2. Bayesian Statistical Analysis

In order to estimate the coefficients and complete the semiempirical relationship for τ_{bf}^* and Re_p , we begin by performing a Bayesian linear regression using equation (5) (see Christensen et al. [2011], for an excellent treatment of these methods). This represents a purely empirical assessment of the relationship between the three principal, physical variables: channel slope, S , median grain size, D_{50} , and bankfull channel depth, H_{bf} . Equation (5) does not explicitly include representation for submerged specific gravity, R , gravity, g , or viscosity, ν . These physical parameters are grouped into the empirical coefficients. This is appropriate insofar as the analyses are limited to siliciclastic sediments in rivers on Earth's surface. Under these constraints, R and g are nearly constant and ν varies by less than an order of magnitude as a function of temperature [Haynes, 2012]. Viscosity should also vary with suspended sediment concentration at bankfull discharge. It could therefore contribute to the overall relationships investigated here, but because it is not included in our data set references, we cannot analyze its effects.

3.3. Data Model

Data from the expanded data set is modeled with equation (5) using Bayesian linear regression. This requires specification of two components in addition to data: a probability distribution for the response variable, S , and a prior distribution for the empirical coefficients that are the focus of interest, α_0 , α_1 , and α_2 . We begin with a common assumption that the response, $\log S$, is normally distributed:

$$\log S_i | \mu_i, \tau \sim \text{independent Normal}(\mu_i, \tau), \tag{9}$$

where $|$ denotes "given" or "conditioned on" and $i = \{1, \dots, 541\}$, is an index for observations in our data set. The above model allows the mean (μ_i) to change across observations (slopes), but it ensures that all slopes have a common precision τ . In addition, the 541 observations on slope are (conditionally) independent. The regression model is a model on the mean,

$$\mu_i = \alpha_0 + \alpha_1 \log D_{50i} + \alpha_2 \log H_{bf i}, \tag{10}$$

which is essentially a statistical formulation based on equation (5).

The prior model is a joint distribution for the four parameters, α_0 , α_1 , α_2 , and τ . Independence priors for all the parameters are assumed [Christensen et al., 2011, section 9.4]. Specifically, this assumption includes a very wide normal distribution for the coefficients of equation (10) and a very wide uniform distribution for the variance of $\log S$ in equation (9), i.e., $\alpha_j \sim \text{Normal}(0, 0.0001)$ for $j = 0, 1, 2$, and $\tau = \frac{1}{\sigma^2}$ where $\sigma^2 \sim \text{Uniform}(0, 1000)$. For both cases, the prior precision is very small, alternatively, the variance is very large; practically, this means that all the priors are very diffuse. This is designed to minimize the impact of the specific choice of priors on the model outcome.

3.4. Model Fitting and Assessing

The posterior distributions for the four parameters cannot be obtained analytically, so Markov chain Monte Carlo (MCMC) methods are used to obtain samples from the distributions. We used the Just Another Gibbs Sampler (JAGS) [Plummer, 2003] package through its interface via R [R Core Team, 2012], rJAGS [Plummer, 2010a, 2010b]. rJAGS includes MCMC algorithms, and this alleviates the need to program one. We

specifically used rJAGS to produce MCMC samples, which were then analyzed using the “coda” package in R [Plummer *et al.*, 2006].

To model the full data set, three MCMC chains with values of 3000 for burn-in, 5 for thinning, and a total of 10,000 iterations were used for generating the samples. Trace plots and autocorrelation plots were both satisfactory given usual descriptions [Christensen *et al.*, 2011, section 6.3.5]. Specifically, the trace plots indicated that the three MCMC samples mixed well in that the starting values did not affect the final state of the chains. The autocorrelations dropped to null values indicating that the sample values were not correlated after the initial burn-in period. In addition, we compared the data on log of slope to median posterior predicted values of log of slope using our model and these fell along a 1:1 line with modest divergence at the highest slope values.

4. Results

4.1. Data Set

Our complete data set now has 541 records from 12 countries and 27 U.S. states (Figure 2); it is available in its entirety in the supplementary online materials. All records include data on slope, median grain size, bankfull channel depth, and original publication source. Multiple published measurements from single and very nearby sites are grouped so that each location exerts equal influence on empirical results. Uncertainty is not uniformly reported from the data sources, so our analyses cannot include rigorous uncertainty propagation. Uncertainty in estimates of the coefficients is specifically a reflection of the scatter in the data and not in the uncertainty from the original measurements and methods themselves. These data come from locations in a wide range of regions and environments thus minimizing possible regional biases. However, there is substantial overrepresentation of North American rivers in the data set because of the availability of data from government agencies. Although this is a shortcoming of the presented data set, it is the best available source for testing relationships between bankfull Shields stress and particle Reynolds number.

These data represent a wide range of climatic conditions, river morphology, and human influence, but the extent to which they represent alluvial channels that are in equilibrium with modern hydrologic and sediment regimes should be addressed here. Although there is no general metric for reporting the degree to which channels are in equilibrium, no streams in this data set were reported in their original sources or are otherwise known to us to be out of equilibrium with modern conditions. This notwithstanding, it is very likely that some channels in this data set are currently out of equilibrium. One possible source of systematic variation away from equilibrium is Quaternary climate and sediment changes associated with glaciation. However, even this has been argued to depend on the time scale of interest and result in both depositional and erosional behavior in fluvial systems [Vandenbergh, 1995, 2003]. Even if there are channels in the data set that are out of equilibrium with modern conditions, it is unclear that nonequilibrium conditions should have a systematic effect on the relationship between bankfull Shields stress and particle Reynolds number across their range of values. Nonetheless, this is an issue that should temper the interpretation of this data set and its analysis.

4.2. Bayesian Analysis

The results of equation (5) regression are summarized fully in Table 1. The regression coefficient that modulates the impact of $\log H_{bf}$ is tightly centered near -1.1 with a 95% high probability density (HPD) interval of $(-1.2, -1.0)$. The coefficient for $\log D_{50}$ has a 95% HPD interval of $(0.22, 0.29)$ and a median of 0.25 , and the 95% HPD interval of the intercept α_0 is $(-2.1, -2.0)$ with a median of -2.1 . The coefficients in equation (8) are functions of those in equation (5); using MCMC methods for estimating the coefficients in equation (5) or alternatively equations (9) and (10), allows us to obtain MCMC chains from the distributions of the coefficients in equation (8), and in effect to estimate the distributions of those coefficients. The 95% HPD interval for the intercept, γ_0 is $(0.95, 1.5)$ with a mean of 1.2 . The median is also 1.2 implying that the posterior distribution is nearly symmetric. This is also the case for the coefficients γ_1 , 95% HDP $(0.0, 0.15)$ with mean of 0.08 , and γ_2 , 95% HDP $(0.48, 0.54)$ with mean of 0.51 . This is consistent with the previous estimate by Wilkerson and Parker [2011], -0.51 , from a smaller data set. Based on our estimates of the coefficients in equation (8), including the intercept, it also fits the data set well. It is important to point out that this does not match the apparent scaling of bankfull Shields stress with particle Reynolds number seen in equation (4). This is because the relationship in equation (4) does not account for the implicit interrelation of channel

slope, bankfull depth, and median grain size. Only by explicitly including their relationship through the empirical equation (5) can coefficients for equation (8) be derived through regression, thus providing an empirical closure and a summary dimensionless relationship for the data set (Figure 2).

5. Discussion and Conclusions

5.1. The Semiempirical Relationship

5.1.1. Effects of Transport Mode

The original conception of the relationship between bankfull Shields stress and particle Reynolds number comprised two stable states for Shields stress, succinctly summarized by *Dade and Friend* [1998] as the following. Rivers with modal sand and silt transport their loads in suspension at bankfull, and the transport proceeds at capacity. In contrast, rivers with modal gravel transport their loads at bankfull as bedload at the threshold of motion (i.e., at competence). It is clear that this conception is partially the result of early, small data sets compounded by the scarcity of rivers with modal grain sizes between very coarse sand and granule gravel. Even in our larger data set, there appear to be two distinct populations of grains separated by the relative scarcity of transitional grain sizes between sand and gravel. The paucity of materials in this size range can be attributed to a minimum in production due to the kinetics of grain impacts. First observed by *Udden* [1914], this grain size gap has been generalized by *Jerolmack and Brzinski* [2010] as an equivalent phenomenon in both aqueous systems (dominantly rivers) and aeolian systems (dominantly dune fields) scaled by their physical properties.

Despite this data gap, the trend of bankfull Shields stress with particle Reynolds number appears continuous across the entire range of grain sizes, and the transition between suspension dominated sand-silt rivers and bedload dominated gravel rivers is smooth (Figure 2). To elucidate this point, Figure 2 includes curves of constant Rouse number, p , calculated in Shields stress-particle Reynolds number space at the transition from pure bedload to partial suspension ($p = 2.5$) and at the transition from partially suspended to fully suspended ($p = 0.8$) [after *Bagnold*, 1973; *van Rijn*, 1984; *Julien*, 1998]. Specifically, Rouse curves are determined by relating shear velocity at bankfull to bankfull Shields stress and sediment fall velocity to particle Reynolds number. The relationship between bankfull Shields stress and particle Reynolds number maintains a continuous slope across these Rouse number predicted transitions in transport mode. Therefore, we argue that, however counterintuitive, transport mode has no threshold effect on the relationship between bankfull Shields stress and particle Reynolds number in alluvial channels.

5.1.2. Implications for Importance of Channel Slope

The relationship in equation (8) appears to depend partially on channel slope, S , although this is somewhat ambiguous because the posterior distribution of coefficient γ_1 , the effect of $\log S$, actually includes zero. In our solution, $\tau_{bf}^* \sim Re_p^{-1/2}$ is potentially a complete scaling relationship between bankfull Shields stress and particle Reynolds number. If, however, channel slope exerts a real influence on this relationship, then the effect is very small across the range of normal alluvial channel slopes. Applying the median of γ_1 , 0.08, to normal slopes, 10^{-3} to 10^{-5} , the slope term in equation (8) varies between 0.24 and 0.40. This equates to a variability of $\pm 30\%$ around the average.

This effect could be real insofar as low sloping rivers carry more washload relative to total load. This would mean that less of the boundary shear stress in these rivers is applied to moving bed-material load and more is applied to transporting sediment that it not represented in the channel boundary. As a secondary control, this potential effect deserves attention, but the data presented here are not an appropriate basis for a thorough analysis.

The results of *Mueller et al.* [2005] and *Parker et al.* [2007] also suggest that bankfull Shields stress depends more strongly on channel slope. Both present linear regressions that appear to fit their data well. However, these regressions do not take into account the simultaneous interrelationships of bankfull depth and grain size with both slope and bankfull Shields stress. Only when the mutual interdependence of all the relevant quantities is investigated can their independent effects be discerned. Specifically, the effect of slope variations on bankfull Shields stress cannot be uniquely determined without simultaneously estimating the effects of bankfull depth and median grain size variations. Because our approach accounts for these combined effects, we conclude that bankfull Shields stress is nearly independent of slope.

5.1.3. Other Potential Factors

There are other important factors that could locally alter this relationship from its global solution—specifically form drag and geomorphic history. Because the theory for this relationship neglects form drag, sources of flow resistance beyond the grain scale are not included (e.g., bed forms, channel planform curvature, in situ vegetation, or large woody debris). To account for this, one would use skin friction shear stress instead of boundary shear stress to compute bankfull Shields stress as in equations (1) and (2). This substitution seems likely to alter the final form of the relationship or at least its coefficients. Although form drag varies systematically with bed morphology [Engelund and Fredsoe, 1982] and bed morphology varies systematically with grain size [Southard and Boguchwal, 1990], there does not appear to be a systematic bias associated with form drag as a function of grain size. Engelund and Fredsoe [1982] suggest that the fraction of flow resistance generated by form drag should have a central maximum in the region of fully developed dunes approaching washout (i.e., near $D_{50} = 0.3$ mm or $Re_p = 30$ in Figure 2). This is not however manifest in the data set.

The data support either of two possible inferences. First, the difference between skin friction shear stress and total boundary shear stress could be small enough across the entire range of grain sizes and transport conditions that form drag ultimately has no detectable effect on the relationship. Alternatively, the effect of form drag could result in systematic, monotonic variation in the relationship between bankfull Shields stress and particle Reynolds number. If this is the case, then the variation of the fraction of resistance from form drag must itself be monotonic. Because upper plane bed (washout) must provide less form drag than dunes, a monotonic increase does not seem reasonable [Engelund and Fredsoe, 1982]. For this reason, we argue that the effects of form drag are not systematic across the data set. Rather, the effects must manifest solely in the variability of the data about the mean trend.

Geomorphic history could also be a factor in some locations. For example, if some locales experienced changes in climate to drier conditions, then a river might have carried materials of larger caliber in the past. This could result in a modern channel bed containing relict grain sizes (i.e., greater than that which the slope and channel depth would predict). Alternatively, occupation of a glacial valley by a modern stream could have the same effect even though the source of the coarse material would be different. Finally, stream capture could either increase or decrease discharge at some location and result in the material transported in the channel to be out of equilibrium with the channel slope and depth. In general, these are non-equilibrium effects, and implicit in the theory is an equilibrium condition. However, it seems highly unlikely that historical factors could systematically alter the effect of $\log D_{50}$ across the entire observed range. It is much more likely that this is responsible for a portion of the large variability in the data set.

5.2. Estimating Paleoslopes

Rivers respond stratigraphically over a variety of scales to changes in external and internal conditions [e.g., Whittaker et al., 2011; Paola and Martin, 2012]. Estimation of surface slopes in ancient alluvial channel systems from measurement of their hydraulic and sedimentologic characteristics is a primary method for reconstructing conditions in these ancient sediment transport systems. Existing methods for determining paleoslopes have been developed using the notion of two stable stress states in alluvial rivers, i.e., all gravel rivers have the same bankfull Shields stress [Paola and Mohrig, 1996]. The relationship in equation (5) provides a new model for investigating paleohydraulic conditions to assess the behavior of ancient rivers. Because of the relative ease with which paleo-flow depths and bed sediment characteristics can be determined, this relationship makes an excellent model for estimating paleoslope from fluvial strata such as is done by McMillan et al. [2002], Heller et al. [2003], Cassel and Graham [2011], Weckwerth [2011], and Duller et al. [2012]. Care should be taken to interpret these paleoslopes as representative of individual river reaches and not as regional surfaces [Engelder and Pelletier, 2013].

There are two results of our analysis that are worth noting in this context. First, slope estimates scale approximately inversely linearly with bankfull channel depths (i.e., $S \sim H_{bf}^{-1.09}$, Table 1) but are relatively weakly dependent on median grain size (i.e., $S \sim D_{50}^{-0.25}$). As a consequence, accurate measurements of paleo-flow depth are critical to successful application of this model to ancient fluvial systems. Based on the posterior distributions of the regression coefficients for equation (5), full error prorogation estimates could be derived but are beyond the scope of the current work.

Second, slope estimates from the model in equation (5) with coefficients from Table 1 are not of equal quality over the entire range of possible alluvial slopes. Rather, estimated slopes appear to match measured

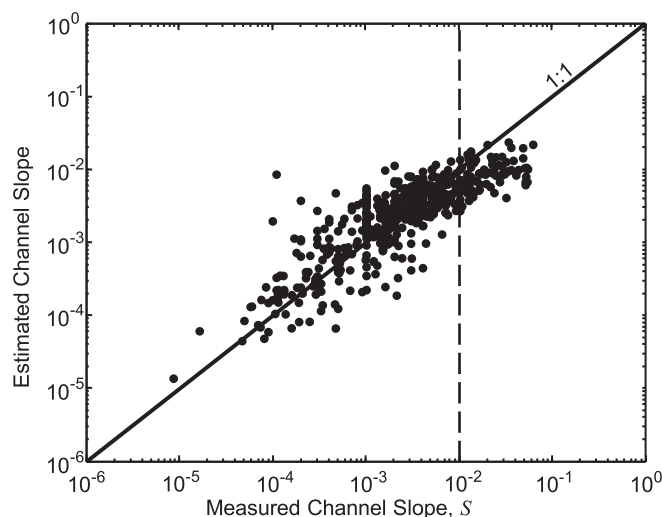


Figure 3. Plot of estimated slopes against measured slopes. Slope estimates are made from measured bankfull depth and median grain size using equation (5) and coefficients in Table 1. The measured and estimated slopes fall on a 1:1 line up to measured slopes of 10^{-2} or estimated slopes of 5×10^{-3} . Above these slopes, the model's accuracy decreases with increasing slope.

slopes only for values of measured slopes gentler than $S = 10^{-2}$ (Figure 3). For the range of slopes steeper than $S = 10^{-2}$, the correspondence of measured and estimated slope values decreases with increasing slope. Based on the pattern of divergence of estimated and measured slopes in Figure 3, we suggest that slope estimates with this method are most reliable at estimated slope values below $S = 5 \times 10^{-3}$.

5.3. Extraterrestrial Application

Application of equation (5) with the coefficients given in Table 1 as a model for organization of alluvial channels requires the assumption of siliciclastic sediments in rivers on Earth. A generalized relationship however should be applicable to a much greater range of channelized

flows transporting detrital materials at low concentrations, including those on extraterrestrial bodies. Relationships for hydraulic geometry are regularly applied to channel-formed deposits on mars [e.g., Williams et al., 2009; Kleinhans, 2010]. We argue that our presented relationship is not yet appropriate for that application because α_0 specifically includes water viscosity, Earth gravity, and the ratio of densities of siliciclastic sediment to water as a single constant. In order to address this issue, variance along the α_0 dimension of the parameter space must be included in an empirical investigation. If this can be accomplished, then estimates of fluid-flow conditions (depth, discharge, etc.) could be made in alluvial channels on extraterrestrial bodies using topography (slope) in combination with character of granular materials. As it currently stands however, equations (5) and (8) are not appropriate for alluvial channels beyond Earth.

6. Summary

In summary, we have provided an expanded data set with which to investigate the organization of alluvial channels with respect to their dominant stresses, materials transported, and hydraulic geometries. By applying a Bayesian regression to an empirical relationship for the primary physical variables, channel slope, bankfull channel depth, and median grain size, we have generated a semiempirical solution for bankfull Shields stress as a function of particle Reynolds number. This relationship varies smoothly across grain sizes and transport modes with $\tau_{bf}^* \sim Re_p^{-1/2}$. This relationship appears to be nearly independent of channel slope. The empirical relationship for slope with bankfull depth and median grain size is appropriate for estimating slopes in ancient channel deposits on Earth, but cannot be applied in its current form to extraterrestrial alluvial systems.

References

- Ackers, P., and W. R. White (1973), Sediment transport: New approach and analysis, *J. Hydraul. Div.*, 99, (11), 2041–2059.
- Bagnold, R. A. (1973), The nature of saltation and of bed-load transport in water, *Proc. R. Soc. London, Ser. A*, 332, 473–504.
- Cassel, E. J., and S. A. Graham (2011), Paleovalley morphology and fluvial system evolution of Eocene-Oligocene sediments ("auriferous gravels"), northern Sierra Nevada, California: Implications for climate, tectonics, and topography, *GSA Bull.*, 123(9/10), 1699–1719.
- Christensen, R., W. Johnson, A. Branscum, and T. Hanson (2011), *Bayesian Ideas and Data Analysis*, Chapman and Hall, Boca Raton, Fla.
- Church, M. (2002), Geomorphic thresholds in riverine landscapes, *Freshwater Biol.*, 47(4), 541–557.
- Dade, W. B., and P. F. Friend (1998), Grain-size, sediment-transport regime, and channel slope in alluvial rivers, *J. Geol.*, 106, 661–675.
- Doyle, M., D. Shileds, K. Boyd, P. Skidmore, and D. Dominick (2007), Channel-forming discharge selection in river restoration design, *J. Hydraul. Eng.*, 133(7), 831–837, doi:10.1061/(ASCE)0733-9429(2007)133:7(831).
- Duller, R. A., A. C. Whittaker, J. B. Swinehart, J. J. Armitage, H. D. Sinclair, A. Bair, and P. A. Allen (2012), Abrupt landscape change post6 Ma on the central Great Plains, USA, *Geology*, 40(10), 871–874.
- Dunne, T., and L. B. Leopold (1978), *Water in Environmental Planning*, W. H. Freeman, San Francisco, Calif.

Acknowledgments

This work was partially supported by the Chevron Energy Technology Company, and the University of Wyoming School of Energy Resources. S.H. was partially supported by the National Science Foundation under Grant DMS-1127914 to the Statistical and Applied Mathematical Sciences Institute. Any opinions, findings, and conclusions or recommendations expressed in this material are those of the author(s) and do not necessarily reflect the views of the National Science Foundation. We would like to thank Editor Montanari, A. Wickert, and anonymous reviewers for very constructive comments. We would also like to thank M. Lamb and G. Parker for fruitful discussions.

- Einstein, H. A. (1950), The bed-load function for sediment transportation in open channel flows, *Tech. Bull.* 1026, U.S. Dep. of Agric, Washington, D. C.
- Engelder, T., and J. Pelletier (2013), Autogenic cycles of channelized fluvial and sheet flow and their potential role in driving long-runout gravel progradation in sedimentary basins, *Lithosphere*, 5(4), 343–354, doi:10.1130/L274.1.
- Engelund, F., and J. Fredsoe (1982), Sediment ripples and dunes, *Annu. Rev. Fluid Mech.*, 14, 13–37.
- García, M. H., E. M. Laursen, C. Michel, and J. M. Buffington (2000), The legend of AF Shields, *J. Hydraul. Eng.*, 126(9), 718–723.
- García, M. H. (Ed.) (2007), *Sedimentation Engineering: Processes, Management, Modeling, and Practice*, 1050 pp., Am. Soc. of Civ. Eng., Reston, Va.
- Hajek, E. A., and M. A. Wolinsky (2012), Simplified process modeling of river avulsion and alluvial architecture: Connecting models and field data, *Sediment. Geol.*, 257, 1–30.
- Harrelson, C. C., C. L. Rawlins, and J. P. Potyondy (1994), Stream channel reference sites: An illustrated guide to field technique, *USDA For. Serv. Gen. Tech. Rep. RM-245*, U.S. Dep. of Agric., For. Serv., Rocky Mt. For. and Range Exp. Stn., Fort Collins, Colo.
- Haynes, W. (Ed.) (2012), *CRC Handbook of Chemistry and Physics*, 2664 pp., CRC Press, Boca Raton, Fla.
- Heller, P. L., K. Dueker, and M. E. McMillan (2003), Post-Paleozoic alluvial gravel transport as evidence of continental tilting in the U.S. Cordillera, *GSA Bull.*, 115(9), 1122–1132.
- Jerolmack, D. J., and T. A. Brzinski (2010), Equivalence of abrupt grain-size transitions in alluvial rivers and eolian sand seas: A hypothesis, *Geology*, 38(8), 719–722.
- Julien, P. Y. (1998), *Erosion and Sedimentation*, 280 pp., Cambridge Univ. Press, N. Y.
- Kleinmans, M. G. (2010), A tale of two planets: Geomorphology applied to Mars' surface, fluvio-deltaic processes and landforms, *Earth Surf. Processes Landforms*, 35(1), 102–117.
- Langbein, W. B., and L. B. Leopold (1964), Quasi-equilibrium states in channel morphology, *Am. J. Sci.*, 262(6), 782–794.
- Leopold, L. B. (1994), *A View of the River*, Harvard Univ. Press, Cambridge, Mass.
- Leopold, L. B., and T. Maddock (1953), The hydraulic geometry of stream channels and some physiographic implications, *U.S. Geol. Surv. Prof. Pap.*, 252, 1–57.
- McMillan, M. E., C. L. Angevine, and P. L. Heller (2002), Postdepositional tilt of the Miocene-Pliocene Ogallala Group in the western Great Plains: Evidence of late Cenozoic uplift of the Rocky Mountains, *Geology*, 30, 63–66.
- Mueller, E., J. Pitlick, and J. Nelson (2005), Variation in the reference Shields stress for bed load transport in gravel-bed streams and rivers, *Water Resour. Res.*, 41, W04006, doi:10.1029/2004WR003692.
- Paola, C., and J. M. Martin (2012), Mass-balance effects in depositional systems, *J. Sediment. Res.*, 82, 435–450.
- Paola, C., and D. Mohrig (1996), Palaeohydraulics revisited: Palaeoslope estimation in coarse-grained braided rivers, *Basin Res.*, 8, 243–254.
- Parker, G. (1978a), Self-formed straight rivers with equilibrium banks and mobile bed. Part 1. The sand-silt river, *J. Fluid Mech.*, 89(1), 109–125.
- Parker, G. (1978b), Self-formed straight rivers with equilibrium banks and mobile bed. Part 2. The gravel river, *J. Fluid Mech.*, 89(1), 127–147.
- Parker, G., P. Wilcock, C. Paola, and W. Dietrich (2007), Physical basis for quasi-universal relationships for bankfull hydraulic geometry of single-thread gravel-bed rivers, *J. Geophys. Res.*, 112, F04005, doi:10.1029/2006JF000549.
- Plummer, M. (2003), JAGS: A program for analysis of Bayesian Graphical Models using Gibbs sampling, paper presented at the 3rd International Workshop on Distributed Statistical Computing (DSC 2003), Austrian Science Foundation, Vienna.
- Plummer, M. (2010a), *JAGS Version 2.00 Manual*. [Available at <http://mcmc-jags.sourceforge.net>.]
- Plummer, M. (2010b), *rJAGS: Bayesian Graphical Models Using MCMC. R Package Version 2.1.0–2*. [Available at <http://mcmc-jags.sourceforge.net>.]
- Plummer, M., N. Best, K. Cowles, and K. Vines (2006), CODA: Convergence Diagnosis and Output Analysis for MCMC, *R News*, 6, 7–11.
- R Core Team (2012), *R: A Language and Environment for Statistical Computing*, R Found. for Stat. Comput., Vienna, Austria. [Available at <http://www.R-project.org>.]
- Rosgen, D. L. (1996), *Applied River Morphology*, vol. 1481, Wildland Hydrol. Books, Pagosa Springs, Colo.
- Southard, J., and L. Boguchwal (1990), Bed configurations in steady unidirectional water flows. Part 2. Synthesis of flume data, *J. Sediment. Res.*, 60(5), 658–679.
- Talling, P. (2000), Self-organization of river networks to threshold states, *Water Resour. Res.*, 36(4), 1119–1128.
- Udden, J. A. (1914), The mechanical composition of clastic sediments, *GSA Bull.*, 25, 655–744.
- van Rijn, L. C. (1984), Sediment transport, Part II: Suspended load transport, *J. Hydraul. Eng.*, 110(11), 1613–1641.
- Vandenbergh, J. (1995), Timescales, climate, and river development, *Quat. Sci. Rev.*, 14, 631–638.
- Vandenbergh, J. (2003), Climate forcing of fluvial system development: An evolution of ideas, *Quat. Sci. Rev.*, 22, 2053–2060.
- Vogel, R., J. Stedinger, and R. Hooper (2003), Discharge indices for water quality loads, *Water Resour. Res.*, 39(10), 1273, doi:10.1029/2002WR001872.
- Weckwerth, P. (2011), Palaeoslopes of Weichselian sand-bed braided rivers in the Torun Basin (Poland): Results of a palaeohydraulic analysis, *Geologos*, 17(4), 227–238.
- Whittaker, A. C., R. A. Duller, J. Springett, R. A. Smithells, A. L. Whitchurch, and P. A. Allen (2011), Decoding downstream trends in stratigraphic grain size as a function of tectonic subsidence and sediment supply, *GSA Bull.*, 123(7/8), 1363–1382.
- Wilkerson, G. V., and G. Parker (2011), Physical basis for quasi-universal relationships describing bankfull hydraulic geometry of sand-bed rivers, *J. Hydraul. Eng.*, 137(7), 739–753.
- Williams, R. M. E., R. P. Irwin, and J. R. Zimbelman (2009), Evaluation of paleohydrologic models for terrestrial inverted channels: Implications for application to martian sinuous ridges, *Geomorphology*, 107, 300–315.
- Wolman, M. G. (1954), A method of sampling coarse river-bed material, *Trans. AGU*, 35, 951–956.
- Wolman, M. G., and J. P. Miller (1960), Magnitude and frequency of forces in geomorphic processes, *J. Geol.*, 68, 54–74.
- Yalin, M. S. (1972), *The Mechanics of Sediment Transport*, Pergamon, Oxford, U. K.